Multi-omic analysis of coral development elucidates the metabolic transitions from parental provisioning to endosymbiotic nutritional exchange

Ariana S. Huffmyer* [1,2], Kevin H. Wong [1,3], Danielle M. Becker [1], Emma Strand [1], Tali Mass [4], Hollie M. Putnam [1]

1. Department of Biological Sciences, University of Rhode Island, Kingston RI 02881 USA
2. School of Aquatic and Fishery Sciences, University of Washington, Seattle WA 98105 USA
3. Rosenstiel School of Marine and Atmospheric Science, Department of Marine Biology and Ecology, University of Miami, Miami FL 33149 USA
4. Department of Marine Biology, The Leon H. Charney School of Marine Sciences, University of Haifa, 3498838, Mt. Carmel, Haifa, Israel

*Corresponding author: Ariana S. Huffmyer; ashuffmyer@gmail.com

Keywords: Montipora capitata, Symbiodiniaceae, metabolomics, transcriptomics, larvae

Running Title: Developmental transitions in coral-symbiont nutritional exchange

Abstract

Anthropogenic climate change threatens the persistence of coral reefs by impacting reproduction and accelerating coral loss. Adult corals depend on nutritional exchange with their endosymbiotic algae (Symbiodiniaceae) to fulfill their energetic demands. However, the mechanisms underlying the onset of this exchange during early life stages and how it contributes to developmental energy demands are unclear. We conducted an integrative analysis of the dependence on nutritional exchange across developmental stages in *Montipora capitata*, a vertically transmitting coral (Symbiodiniaceae are passed from parent to offspring) in Hawai□i. We applied physiological (metabolism and symbiont density) and multi-omic (metabolomics, transcriptomics, and microbial amplicon sequencing) approaches over 13 time points (1-255 hours post-fertilization; eggs, embryos, larvae, and recruits) to understand ontogenetic shifts in metabolism. Energetic demand (respiration) and symbiont population photosynthetic capacity (photosynthesis and cell density) increased with development, and metabolism shifted from using stored reserves to relying on symbiont-derived resources. Specifically, pathways associated with nutritional exchange, including organic compound transport, glucose and fatty acid metabolism, nitrogen metabolism, and reactive oxygen regulation were enriched in larvae. Recruits expanded utilization of carbohydrate and lipid pathways in response to the energetic demands of settlement and calcification. Our study shows that symbiotic nutritional exchange buffers the energetic demands of development in vertically transmitting corals, suggesting that in environmentally stressful conditions, these stages may be increasingly vulnerable to the loss of symbiont-derived nutrition. Therefore, intervening early to reduce stress during sensitive developmental stages could enhance coral reef recruitment and recovery as climate change intensifies.

Introduction

Symbiotic relationships between animals and microbial organisms enable survival in nutritionally challenging environments (1). The function and structure of one of the most ecologically and economically important ecosystems on Earth, coral reefs, is driven by the productivity of marine symbioses. The nutritional symbiosis between reef-building corals and endosymbiotic algae in the family Symbiodiniaceae (2) can provide >100% of the coral's daily metabolic demands through translocated organic carbon compounds generated via symbiont photosynthesis (3, 4). In return, metabolic waste from the coral host, including nitrogen and inorganic carbon, is provided to the Symbiodiniaceae to support growth and metabolism (5, 6). The energy-enhancing nutrient exchange between Symbiodiniaceae and corals, as well as a diverse bacterial and archaeal microbiome (7), enables calcium carbonate production and thus the 3D skeletal structure that provides a habitat for high biodiversity (8) and invaluable goods and services (9). However, this delicate symbiosis is susceptible to destabilization by environmental stress. Rising sea surface temperatures and acute marine heat waves cause coral bleaching, or the dysbiosis and loss of symbionts and their carbon surplus from the coral (10), which can, and often does, culminate in mortality at reef-wide levels (11). Increasingly, the stability and persistence of the nutritional relationship between corals, their algal endosymbionts, and symbiotic microbes are critical for the continued survival of reefs and the maintenance of essential ecosystem services that coastal communities rely on.

Globally, half of the live coral cover has been lost since the 1950s (12), significantly increasing the importance of coral reproduction and recruitment to replenish and maintain reef ecosystems. Corals have complex and biphasic life cycles, in which adults produce gametes that are internally or externally fertilized and develop into swimming larvae that then undergo metamorphosis into the sessile polyp recruit stage and grow into mature colonies (13). Survivorship from fertilization to recruitment represents the primary bottleneck for marine larvae (14), due to environmental impacts on fertilization, larval dispersal and behavior, predation, and substrate suitability (13). Key among the myriad challenges facing these sensitive life stages is the energetic requirement for successful development, homeostasis, and metamorphosis (15). To buffer these challenges, corals form associations with Symbiodiniaceae either immediately through vertical transmission (i.e., symbionts are provisioned to the eggs), or within days to weeks of release and/or settlement through the process of horizontal transmission (i.e., symbionts are acquired from the environment) (16). Initiation of symbiosis is a topic of intense study (17), but the successful establishment of the nutritional exchange, or symbiotic integration, in early life history remains less well understood despite its increasing importance to reef persistence and recovery.

The establishment of nutritional symbioses in early life history has direct implications for coral survival. Without symbiotic nutritional sources, coral embryos and larvae initially rely on limited endogenous lipid reserves in the forms of phospholipids (primarily for use in cell membranes), wax esters (most abundant class available as fatty acid reserves for metabolic oxidation), and triacylglycerols (storage lipids that can be rapidly metabolized) (18). Furthermore, there are conflicting findings on the capacity of the coral-algal symbiosis to contribute substantially to the energetic demands of early life stages. For example, high-performance thin-layer chromatography lipid analysis in aposymbiotic larvae indicates a decline in wax ester abundance as larvae age, with a strong reliance on parentally provisioned fatty acids for energetic fuel (19). In symbiotic larvae, this demand for energy reserves can be supplemented by symbiotic nutrition, observed as carbon translocation (20) and reduced rates of lipid depletion under light conditions (21). In contrast, stable isotope pulse-chase and nanoscale secondary ion mass spectrometry (NanoSIMS) imaging in symbiotic larvae indicate that nutritional exchange is possible, but substantially lower relative to levels of exchange at the adult stage (22), highlighting the need for ontogenetic and mechanistic studies to resolve the role of symbiotic nutrition in contributing to recruitment costs. However, heavy reliance on nutritional exchange during early life history can increase susceptibility to climate change stressors, such as light driven increases

in cellular damage due to the presence of symbionts (23). As thermal stress increases, bleaching and symbiotic disruption could destabilize nutritional exchange and worsen recruitment bottlenecks. Further, it has been hypothesized, but not yet tested, that nutritional exchange plays a more important role in metabolism as development progresses through metamorphosis and settlement (22, 24). Therefore, to understand how symbiont-derived nutrition affects coral recruitment under ocean warming, it is important to track metabolism and how nutrients are exchanged across life stages. This requires studying the metabolic changes at molecular and metabolomic levels that occur as corals shift from relying on nutrients provided by their parents (e.g., metabolism of wax esters and storage lipids) to those provided by symbionts (e.g., glucose metabolism and transport of organic compounds).

Considering the critical need to increase our understanding of coral recruitment, we took a cross-scale approach integrating physiological, molecular, metabolomic, and microbiome data of symbiotic performance and nutritional exchange longitudinally across early life history stages of the vertically transmitting coral, *Montipora capitata*, from eggs through metamorphosed and attached recruits (Fig 1AB). We found that (i) energetic demands increase with ontogeny, peaking at metamorphosis; (ii) endosymbiont density and photosynthetic function increase, while Symbiodiniaceae community diversity remains stable and bacterial community diversity increases; and (iii) larva demonstrate shifts in metabolism from parentally provisioned lipids to symbiont-derived carbohydrate and lipids that promote energetic enhancement through the vulnerable transitions of metamorphosis and settlement. This comprehensive characterization of early life history transitions in metabolism demonstrates that energy demands can be buffered by symbiotic nutritional exchange and identifies ontogenetic windows that are vulnerable to dysbiosis because of climate change stressors.

Results and Discussion

A. Energetic demands of development, metamorphosis, and settlement can be buffered by endosymbiont productivity

Progressing through development is an energetically demanding process (25, 26), but it has been debated whether symbiotic nutritional exchange meaningfully contributes to these requirements. To address this, we tracked energy demand (light-enhanced dark respiration) and symbiont carbon fixation (gross photosynthesis) across stages in embryos, larvae, and metamorphosed polyps (65-231 hours post fertilization, hpf) (Fig 1A). There was significant morphological variation in size as embryos developed followed by growth in the larval stage (Kruskal-Wallis, $\chi^2(9,563)=266.37$, $P<0.001$; SI Appendix, Fig S1). Across this time series, individual-normalized respiratory demand significantly increased to be 82-180% higher in polyps than in swimming larvae (Kruskal-Wallis, $\chi^2(5,93)=69.3$, $P<0.001$) (Fig 1C). This is consistent with observations of an 83% increase in post-metamorphosis respiration in Pocilloporid recruits relative to larvae (27). As energetic costs increase with ontogeny and existing reserves are depleted (18), symbiont-derived and/or heterotrophic supplementation becomes essential to support continued development and ultimately survival.

In vertically transmitting corals, the presence of symbionts at these energetically demanding life stages provides the capacity for nutritional supplementation of parental provisions (21). Our cross-stage measurements of symbiont photosynthesis rate in embryo, larval, and metamorphosed polyps (65-231 hpf) (Fig 1A) revealed an average increase of 76% from earliest to latest stages (Fig 1C; Kruskal-Wallis, $\chi^2(5,93)=32.1$, $P<0.001$). This substantial increase in primary production corresponded with reduced energetic capacity (quantified as photosynthesis:respiration ratio) and higher post-metamorphosis metabolic demand (44-58% higher respiration compared to larvae that remained swimming) (Fig 1C; Kruskal-Wallis, $\chi^2(5,93)=38.7$, $P<0.001$). The increased rates in photosynthesis can partially be attributed to proliferation rates of the symbiont population, with density peaking in metamorphosed and settled polyps (Fig 1D; ANOVA, SS=1.02e8, $F(9,30)=25.06$, $P<0.001$). Increased photosynthetic activity

coupled with symbiont population growth indicate larvae have enhanced potential for nutritional contribution from the symbionts through the production of fixed carbon products (4). The disproportionate enhancement in photosynthetic capacity (76%) relative to symbiont cell population growth (34%) (Fig 1CDE) suggests higher photosynthetic capacity on a cell-specific level, which could result from greater photopigment concentrations and/or increased supply of inorganic carbon from host respiration (Fig 1C) as development progress (6, 28), resulting in enhanced capacity for photosynthate generation and translocation (29).

Shifts in photosynthetic function and holobiont performance have been attributed to changes in symbiont community composition in adult *M. capitata* (30, 31). A mixture of *Cladocopium* sp. and *Durusdinium* sp. is characteristic of this species in Kāne□ohe Bay, Hawai□i (30, 32). Considering this, we tested the hypothesis that the genetic identification of Symbiodiniaceae changed with ontogeny. There was no effect of life stage on Symbiodiniaceae ITS2 profile (Defining Intragenomic Variant (DIVs); (35)) community similarity (PERMANOVA, SS=0.360, R^2=0.261, F(9,28)=1.098, *P*=0.217; SI Appendix, Fig S2A) and alpha diversity did not change across ontogeny (Kruskal-Wallis, χ^2(9,28)=9.541, *P*=0.389; SI Appendix, Fig S2B), indicating stable symbiont communities in early life history. Our samples contained both *Cladocopium* sp. (ITS2 Profile C31.C17d.C21.C21ac.C31a; (33)) and *Durusdinium glynnii* (ITS2 Profile D1.D4.D6.D1ab.D17d; (34)), with a majority of the former (55.9±0.8% and 44.1±0.8%, respectively) (SI Appendix, Fig S2C). However, as environmental conditions continue to change (e.g., chronic temperature stress, acute heat waves increase), the thermal tolerance of *D. glynnii* previously documented in adult *M. capitata* (36, 37) could manifest in a shift to a greater abundance of *D. glynnii* than *Cladocopium sp.* provisioned to offspring (38). Since *D. glynnii* translocates lower amounts of photosynthates than *Cladocopium sp.* in *M. capitata* (29), this could result in detrimental impacts on nutritional availability for offspring in the future. Our results indicate no evidence of winnowing or selection of symbiont partners with ontogeny in *M. capitata* and indicate that increased photosynthetic capacity with age is driven by the growth and physiology of a stable, mixed *Cladocopium* sp. and *D. glynnii* symbiont population.

Holobiont function is driven by metabolic linkages and nutritional cycling between the host and symbiont, and the associated microbial communities (39, 40), but the nutritional relationships between corals and associated bacteria across ontogeny has not been elucidated. Previous work found that nitrogen was translocated between *Pocillopora damicornis* larvae and associated bacteria and was subsequently incorporated into Symbiodiniaceae populations, illustrating microbial influences on nutritional functionality (41). We characterized bacterial communities in *M. capitata* to test the hypothesis that shifts in bacterial associations co-occur with ontogenetic shifts in metabolism. Indeed, bacterial communities varied significantly across ontogeny (PERMANOVA, SS=4.879, R^2=0.643, F(7,17)=4.378, *P*=0.001; SI Appendix, Fig S3A), with alpha diversity peaking during metamorphosis and recruitment (One-way ANOVA; Shannon: SS=20.247, F(7,17)=22.31, *P*<0.001; Inverse Simpson: SS=1.69e4, F(7,17)=17.46, *P*<0.001) (SI Appendix, Fig S3B). This pattern was also observed in the bacterial diversity of *Coelastrea aspera,* which increases from recruit (<6 cm colony diameter) to adult colonies (>28 cm in colony diameter), suggesting community succession with ontogeny (42). In our study, Alteromonadaceae (*Alteromonas* sp.), *Vibrio* sp., and Pseudoalteromonadaceae (*Psychrosphaera* sp.) peak early in development followed by Oceanospiriliaceae (unclassified) increasing in mid-development (SI Appendix, Fig S3CD). In late development, the relative abundance of Rhodobacteraceae and Flavobacteriaceae increases (SI Appendix, Fig S3CD). These taxa play a role in carbon (43), nitrogen (41), sulfur (e.g., DMSP/DMS; (44), and micronutrient cycling (45) along with the production of antimicrobial compounds (46) and, therefore, we hypothesize that an increase in bacterial diversity could confer increased nutritional functional diversity for the host (47, 48). Quantitative measures of nutritional production and cycling in bacterial communities across ontogeny should be completed in future studies with approaches such as metatranscriptomics, DNA-stable isotope probing (e.g., DNA-SIP), as well as metabolomic stable isotope probing and microscopy techniques (e.g., NanoSIMS) to test this hypothesis (49).

B. Transitions from parentally provisioned lipid metabolism to symbiont-derived carbohydrate and lipid metabolism contribute to developmental energy demands

Adult corals meet their energy needs through nutritional exchange with Symbiodiniaceae (3). However, it is unclear how this exchange is initiated in early life stages and when the transition from using parental reserves to relying on symbiont resources occurs. Previous work has examined nutritional exchange only in the larval stage or at a discrete time point and focuses primarily on brooding species (21, 22). To improve our knowledge of these early symbiotic relationships, we studied the metabolic and molecular mechanisms of nutrient exchange across different life stages in a longitudinal approach across development. We characterized gene expression and metabolomic patterns through TagSeq (50) and liquid chromatography–mass spectrometry (LC–MS) metabolomics profiling (*sensu;* (51)), respectively, and assessed these data via weighted co-expression network (WCNA; (52), and functional enrichment analyses (GOSeq Biological Processes ontology, $p<0.001$; MetaboAnalyst, $p<0.05$). Strong gene expression (PERMANOVA; SS=3.18e5, R^2=0.751, F(9,28)=9.362, *P*=0.001; SI Appendix, Fig S4A) and metabolic (PERMANOVA; SS=5.39e3, R^2=0.644, F(12,34)=5.122, *P*=0.001; SI Appendix, Fig S4B) temporal signatures were seen across ontogeny. Based on separate gene (Fig 2AB) and metabolite (Fig 3AB) network analyses, both genes and metabolites displayed three ontogenetic patterns: i) decreasing across development, ii) peaking in mid-development, and iii) increasing across development. Collectively, the results of the gene and metabolite enrichment in each of these three patterns support increased metabolism of symbiont-derived nutrition corresponding to the timeline of increased energy demand, which we describe below.

i. Early development: parentally derived metabolic building blocks

Parentally provisioned transcripts and macromolecules provide the molecular capacity and energy required for rapid cell proliferation and growth during coral embryonic development (53). In early development, embryos undergo a reorganization of tissues and cellular structures, gastrulation and differentiation of germ layers, and rapid cell proliferation. These processes require structural molecules and metabolic building blocks (e.g., glycogen, amino acids, lipids) and capacity for cell signaling and transport (54, 55). However, it is unclear when early life stages of corals transition from utilizing these parental reserves to relying more heavily on symbiont-derived nutrition. In this study, we characterized metabolic and molecular functions in fertilized eggs (1 hpf), cleavage (5 hpf), and mid (38 hpf) to late gastrula (65 hpf) stages, encompassing the maternal to zygotic transcriptional transition previously identified in this species (53) and seen here between expression at 38 and 65 hpf (SI Appendix, Fig S4A). Throughout *M. capitata* embryonic stages, we observed strong signals of the utilization of parentally provisioned energy reserves including lipid and carbohydrate reserves. Specifically, there was enrichment of genes involved in the metabolism of amino sugars and simple carbohydrates (Fig 2C) and lipids (lipid catabolic process) and activation of immune and apoptosis regulation systems (regulation of kappaB, NF-kappaB, and hippo signaling) facilitated by cell signaling (G-protein coupled receptor regulation, signal transduction regulation, steroid metabolism) and transport (organic substance and amino acid transport and ion transport) (Fig 2DE). Further, there was an accumulation of metabolites that result from the catabolism of stored carbohydrates (monosaccharides, tricarboxylic cycle acids) and derivatives (glycosyl compounds) (Fig 3C), with metabolomic enrichment of pathways that generate metabolic coenzymes and dinucleotides (NAD+/NADH; nicotinate and nicotinamide metabolism; Fig 3D).

These findings demonstrate that the energy demand of cell proliferation and signaling functions during embryonic development is met by parentally provisioned reserves with limited evidence for symbiotic nutritional exchange. These results are supported by previous observations of lipid and simple carbohydrate metabolic processes in aposymbiotic larvae (56). Under environmental stressors, maintaining energetic homeostasis in adult tissues reduces the energy available for gamete provisioning (57), which may compromise coral capacity to supply sufficient resources to offspring in subsequent reproductive events following stress (58).

ii. Mid-development: initiating nutritional exchange and regulating symbiosis

Research comparing lipid use in aposymbiotic (horizontal transmitters) and symbiotic (vertical transmitters) larvae indicates that symbiont-derived nutrition can be utilized in the first week of life (19). However, the timing of the metabolic shift from parental reserves to symbiont-derived resources and the extent of its contribution are unclear. Specifically, of the lipids consumed in a spawned aposymbiotic larvae, 26% of these are consumed in the first 3 days of life, while in brooded symbiotic larvae, it takes twice the time for only 16% of their lipid reserve consumption to occur (19). It is possible the lower lipid consumption in the brooded symbiotic larvae reflects the cost savings from already completing the intense demands of cell division for development. In contrast, our data indicate that in a vertically transmitting spawning coral, symbiotic nutrition can supplement stored lipid reserves to support developmental processes, and thus the longevity of lipid stores and potential pelagic duration could be extended. The initial signatures of metabolism of symbiont-derived nutrition are clearly present by mid-development (65-163 hpf) in *M. capitata* ontogeny (Fig 2CDE). In the coral-Symbiodiniaceae symbiosis, metabolites transferred from symbionts to the coral host produced through photosynthesis include glucose, glycerol, galactose, amino acids, fatty acids, and organic acids (59–62). In *M. capitata*, enrichment of genes peaking during the swimming larval stages (93-183 hpf) revealed processes involved in glucose and fatty acid metabolism and enrichment of metabolic derivatives of lipids and carbohydrates. This indicates that concurrent with increased symbiont density and photosynthetic rates, these larvae have the molecular machinery and metabolic capacity to utilize photosynthates.

Glucose, a major metabolite involved in nutritional transfer between symbiont to host (63), is one of the first metabolites utilized by the host at the onset of host-symbiont nutritional exchange in this study. In mid-development, genes involved in glucose and monosaccharide metabolic processes (Fig 2C) are enriched along with metabolite derivatives of tricarboxylic acid cycle metabolism (Fig 3C) resulting from glucose metabolism. To facilitate the translocation and metabolism of carbohydrates, carbohydrate derivative transport and carboxylic acid and organic acid transmembrane transport are active in larval stages (Fig 2E). Utilization of carbohydrates in larval stages supports prior observations that symbiotic larvae use stored reserves at lower rates due to the added energy supplement from symbiont photosynthates (21).

Fatty acids are energy-rich compounds that are largely acquired from the symbiont (e.g., saturated and polyunsaturated fatty acids, docosahexaenoic acid, arachidonic acid, and palmitic acid) (64, 65). However, the role of symbiont-derived fatty acids in supporting developmental costs in the early life history of symbiotic corals is not well understood. In adult corals, fatty acids translocated from the symbionts can be directly metabolized through beta-oxidation in the epidermis, and, simultaneously, excess translocated glucose can be used to synthesize fatty acids in gastrodermis cells and subsequently stored as neutral lipids or wax esters for later use (66). Our data indicate that both processes are occurring in larval stages. First, there was enrichment in fatty acid oxidation (Fig 2D) along with metabolomic enrichment of fatty acids and conjugates and short-chain acids and derivatives (Fig 3C), suggesting that fatty acids from the symbiont are translocated, evidenced by enrichment of organic acid transmembrane transport, and directly metabolized (Fig 2DE). Second, genes involved in fatty acid derivative biosynthesis and positive regulation of lipid biosynthetic processes were enriched, demonstrating that the host is also synthesizing fatty acids from carbohydrate sources and building stored reserves (Fig 2D). Throughout ontogeny, genes involved in lipid metabolism and regulation and lipid catabolism are enriched, indicating continual utilization of stored lipid reserves to support developmental costs (Fig 2D) (19, 21). Because the metabolism of one class of storage lipids, triacylglycerides, does not emerge until late development (described below), lipid metabolism in mid-development is most likely from the catabolism of wax ester stores, which is the largest lipid fraction in coral tissues and the primary lipid energy source in larvae (18, 19). As the contribution of photosynthates increases translocated fatty acids, these compounds may be utilized to rebuild depleted wax ester stores as development progresses. Our understanding of ontogenetic shifts in

lipid translocation and utilization would be improved by the characterization of lipid classes and fatty acid profiles (e.g., (67)) across life stages in vertically transmitting species.

Nitrogen cycling is a critical component of maintaining a stable symbiotic state, since active host nitrogen limitation to the symbionts can enhance the translocation of excess photosynthetically fixed carbon back to the host (5, 28, 68). These processes are at play in early life stages, for example, in brooded *P. damicornis* larvae, exposure to increasing ammonium conditions resulted in increased symbiont population growth (20) and nitrogen transfer has been observed between the larval host and associated bacterial and Symbiodiniaceae communities (41). However, the role of nutrient cycling in establishing symbiotic nutritional exchange across early life history stages has not been characterized. Critically, our data demonstrate that nitrogen cycling occurs during periods when symbiotic nutritional exchange is initiated. Specifically, in mid-development at the swimming larval stages, there was enrichment in alanine, aspartate, and glutamate metabolic pathways (Fig 3D). This observation indicates that nitrogen acquisition via ammonium assimilation into amino acids is occurring through the sequential activity of glutamine synthetase and glutamine synthase. These results are consistent with previous observations that this pathway contributes to nitrogen uptake and subsequent recycling between the host and symbiont (69) and is seen also by its upregulation in symbiotic cnidarians (*Aiptasia* sp.; (66)).

As metabolic activity increases to fuel developmental demands and photosynthetic rates increase with Symbiodiniaceae cell density, we observed that larvae employed reactive oxygen species (ROS) metabolism and management of cellular stress, indicated by enriched gene functions for regulation and metabolism of ROS and immune and stress response signaling (terpenoid and sphingolipid metabolism, protein kinase B signaling) (Fig 2E) (17, 70–72). These results demonstrate that the metabolic transition towards increased utilization of symbiont-derived nutrition begins in larval stages in *M. capitata* and therefore represents a critical period of development that could be energetically sensitive to symbiotic disruption and dysbiosis. Previously, it has been hypothesized that early nutritional exchange has negligible contributions to organismal metabolic demand in larval stages relative to the contributions at adult stages (22). In contrast, our data suggest a key role for symbiont-derived products by mid and late development, even if they are generated and translocated at lower levels than in the adult.

iii. Late development: integrating metabolism to meet energetic demand

In late development (metamorphosis and attached recruits; 183-255 hpf), host-symbiont metabolic interaction increased, demonstrating a greater contribution of symbiont-derived nutrition to support the energetic demands of metamorphosis and settlement. Our data indicate utilization of carbohydrate photosynthates, specifically glucose and galactose (63, 73), in late developmental stages supported by enrichment of glucose, hexose, and monosaccharide metabolism, catabolism, and biosynthesis genes (Fig 2C), monosaccharide and galactose metabolism metabolites (Fig 3CD) and the transport of organic compounds (Fig 2E). Our finding that gene expression and metabolism increased concurrent with elevated symbiont photosynthesis are aligned with previous observations that carbohydrate metabolism and transport genes are upregulated during the day in adult tissues of the confamilial species *Acropora cervicornis* when photosynthetic activity is highest (74). However, there is variability by species and life stage in metabolism and carbohydrate usage dependent on diel cycles and energetic priorities (e.g., investment in calcification or reproduction) (75, 76). Shifts in carbohydrate utilization should be examined across life stages in the context of energy demands in future work.

Complex carbohydrates were also metabolized in attached recruits indicated by enrichment of disaccharide metabolites and starch and sucrose metabolic pathways (Fig 3CD) in addition there was usage of stored carbohydrates demonstrated by enrichment of glycogen, cellular glycan, and glucan metabolism genes (Fig 2C), which are known to be provided by the symbiont and/or generated through the metabolism of stored lipids (77, 78). Our results

demonstrate that the post-settlement energetic demand requires the utilization of translocated and stored sources of carbohydrates in *M. capitata* late developmental stages. This supports previous hypotheses by (22, 24) that nutritional exchange is more meaningful to post-settlement energy demand than in larval stages. This is also consistent with observations that under other energetically stressful conditions, such as thermal stress bleaching, pools of both simple and complex carbohydrates are depleted (77, 79). Additionally, utilization of carbohydrate resources in attached recruit stages may be in response to energy requirements of early calcification. Indeed, in late development, there was upregulation of inorganic ion and cation import across plasma membranes (Fig 2E), which transport ion substrates (e.g., bicarbonate) to the site of calcification (80). Another indicator that nutritional exchange is occurring in attached recruits is through the enrichment of phenylalanine, tyrosine, and tryptophan metabolism (Fig 3D), which are essential amino acids translocated from the symbiont (81) and facilitated by amino acid transmembrane transport genes (Fig 2E) (66).

Similarly, we found evidence that both translocated (fatty acids) and stored lipids (triglycerides and wax esters) are important energy sources during metamorphosis and settlement (Fig 2D) (60). Fatty acid beta-oxidation and metabolism genes (Fig 2D) continued to be expressed corresponding to the enrichment of short chain acids and derivative metabolites (Fig 3C) and genes involved in organic acid transport (Fig 2E). Notably, the enrichment of genes involved in triacylglycerides (also referred to as triglycerides), emerged in late development (i.e., triglyceride metabolic process) (Fig 2D). In several studies (18, 19, 21), triacylglycerols are present and metabolized in symbiotic larvae, but not in aposymbiotic larvae, and is therefore an indicator that symbiont-derived lipid products are synthesized into triacylglyceride stores in the host and used to meet energy demand. Continued enrichment of lipid metabolic processes and neutral lipid metabolism (Fig 2D) indicates that wax ester stores are simultaneously metabolized to support late developmental stages. The capacity to supplement energy demand with symbiotic nutrition can extend the period of lipid catabolism during larval stages, potentially expanding pelagic duration, survival, and dispersal potential in vertical transmitters (21).

The enhancement of products for increased metabolic demands is not, however, without its dangers (23, 82). For example, ROS damage and transcriptional responses have been seen in symbiotic *Acropora intermedia* larvae (144-216 hpf) under increased temperatures (83), corresponding to the stages where we observed enrichment in ROS regulation in mid and late developmental stages (65 through 231 hpf). Specifically, ROS regulation, sphingolipid and ceramide metabolism, and sterol transport genes were expressed in late development (Fig 2E), which have been shown to assist with mitigating cellular stress and increasing membrane stability (71, 72). In addition to redox balance challenges and free radical repair, increases in energetic stress during metamorphosis and recruitment may also enable pathogenic infections (84). We documented enrichment in anti-microbial metabolic pathways (i.e., neomycin, kanamycin, gentamicin biosynthesis) (39, 85, 86) in recruits, which may result from defense to pathogenic infections and/or defense against benthic microbial communities during settlement (87). These results demonstrate that metabolic interaction and integration between the host and Symbiodiniaceae increases in late development, representing an ontogenetic window that relies heavily on the input of symbiotic nutrition in vertically transmitting species to progress through the costly process of metamorphosis and settlement.

C. Conclusions

As climate change stressors increase, successful reproduction and recruitment is critical for coral reefs to persist. Because development is energetically demanding, access to symbiont-derived resources could buffer these costs. However, the contribution of symbiotic nutritional exchange to development has been debated and the ontogenetic shifts in host-symbiont metabolic interactions is unclear. Our integrative and multi-omic approach across an ontogenetic time series in *M. capitata* revealed that in larval stages, symbiont-host nutritional exchange begins, followed by increased utilization of photosynthetic products through metamorphosis and

settlement (Fig 4). We documented increased diversity in the associated bacterial communities across ontogeny that suggest enhanced holobiont functionality and microbial interaction through settlement. Increased metabolic interaction and complexity in attached recruits, evidenced by the metabolism of both stored and symbiont-derived carbohydrates and lipids, shows that symbiotic nutrition is an important energy source as early life stages progress through settlement (Fig 4).

We demonstrate that the energetic costs of development and demands against the limited bank of energy reserves can be buffered by symbiont-derived nutrition in vertically transmitting corals, especially in post-settlement stages and could outweigh energetic vulnerabilities to symbiotic light stress (23). However, in horizontal transmission, the dominant reproductive strategy in reef-building corals (16), the metabolic contribution of symbiont-derived nutrition will depend on the timing of symbiont acquisition ranging from larval to recruit stages (24). As developmental costs increase with climate change (15), access to symbiotic nutrition earlier in development may provide energetic advantages in horizontal transmitters. Reducing environmental stress during the larval and post-metamorphosis when nutritional exchange is being established and is essential contributing to high energy requirements could be a key intervention to enhance recruitment and post-settlement survival on reefs.

Materials and Methods

All raw and processed data and bioinformatic and statistical code are archived openly and are available at https://github.com/AHuffmyer/EarlyLifeHistory_Energetics/releases/tag/v1.0.0 and Open Science Framework (88). Raw sequence files are stored on the NCBI Sequence Read Archive under project PRJNA900235.

A. Gamete collection and developmental rearing

Montipora capitata is a hermaphroditic broadcast spawning, vertically transmitting coral species that is a dominant reef-builder in Kāne□ohe Bay, O□ahu, Hawai□i where this study was conducted (Fig 1B). During the July 2020 spawning period, *M. capitata* egg and sperm bundles were collected on the night of the new moon (21:00 h) by scooping spawned bundles from the surface of the water in Kāne□ohe Bay. Bundles were then transported to the laboratory at the Hawai□i Institute of Marine Biology (HIMB), fertilized at 27.5°C and added to 20 L conical rearing vessels (N =30) supplied with 1 µm filtered seawater (FSW) at 27.5°C and <50 µmol photons m^{-2} s^{-1} (photosynthetic active radiation; PAR) (Fig 1B). Embryos were reared in conical vessels through development to the swimming larval stage (Fig 1B). At approximately 165 hours post-fertilization, larvae were transferred in 53 µm mesh-bottom plastic bins to outdoor flow-through seawater tables for settlement containing aragonite settlement plugs (circular surface; 2.85 cm^2) conditioned for 3 days in seawater. Settlement was conducted at ambient temperature (~28°C) and light of <100 PAR. Two settlement states were sampled in this study - larvae that metamorphosed and attached to the surface of aragonite plugs (Fig 1B) and those that metamorphosed without attachment (i.e., metamorphosed polyps). We sampled time points across the early life history of *Montipora capitata* including fertilized eggs (1 hour post-fertilization, hpf), embryos (cleavage at 5 hpf, late gastrula stage at 38 and 65 hpf), larvae (93, 163, 183, 231 hpf), metamorphosed polyps (83 and 213 hpf), and attached recruits (183, 231, and 255 hpf) (Fig 1A) for molecular, metabolomic, physiological, and amplicon sequencing assays. Detailed methods for this study are described in SI Appendix, Supplementary Methods.

B. Respirometry

Respiration (oxygen consumption) and photosynthesis (oxygen production) rates were measured using an Oxy-10 Sensor Dish Reader (PreSens Precision Sensing) in combination with a 24-well microplate (80 µL; Loligo Systems) at six time points: embryos (65 hpf), larvae (93, 183, and 231 hpf) and metamorphosed polyps (183 and 231 hpf) (Fig 1A). Six individuals were added to each microplate well filled with 1 µm FSW and sealed with glass coverslips. Oxygen production

(photosynthesis) was first measured under light conditions (~500 PAR) followed by measurement of light-enhanced dark respiration (LEDR, hereafter referred to as "respiration"). All measurements were conducted at 28°C. Light levels during photosynthesis measurements are within the saturating irradiance for adults of this species (89), but photosynthesis-irradiance curves were not conducted at the early life stages and therefore, we only focus on relative comparisons between life stages in this study. Photosynthesis and respiration rates were extracted using localized linear regressions and calculated as nmol O_2 individual^{-1} min^{-1}. Photosynthesis:respiration ratios (P:R) were calculated as gross photosynthesis divided by respiration. Normality of residual and homogeneity of variance were assessed using quantile-quantile plots and Levene's tests in the *car* package, respectively (90) in R Statistical Programming v4.2.2 (91). Metabolic rates were then analyzed using non-parametric Kruskal-Wallis tests with time point as the main effect.

C. Size and symbiont cell density

At each time point (Fig 1A), individuals were collected across multiple rearing vessels (*n* = 3-5 conicals or bins), pooled, fixed in 4% paraformaldehyde for 24-36 h then stored in 70% ethanol at 4°C (*n* = 4 samples per time point; approx. 100 individuals per sample) for size and symbiont density measurements. Samples were digitally photographed using a dissecting light microscope with a stage micrometer. Size was calculated as the volume of randomly selected individuals (*n* = 15) from each sample in ImageJ (92). We did not measure the size of attached recruits on plugs because recruits often settled in aggregation, preventing measurement of individual size. We tested for differences in size between life stage time points using a non-parametric Kruskal Wallis test.

Symbiont cell density at each developmental time point (Fig 1A) was measured by conducting replicate cell counts (n = 6-8) of homogenized tissue using a hemocytometer and normalizing to the number of individuals in the sample (egg through metamorphosed polyps; cells individual^{-1}), or total surface area of tissue sampled (attached recruits; cells mm^{-2}). Symbiont densities were analyzed using a one-way ANOVA test with developmental time point as the main effect. Differences in symbiont cell densities between time points in attached recruits (symbiont cells per mm^2) were analyzed separately using a non-parametric Kruskal Wallis test.

D. Gene expression in the coral host

Samples were preserved in DNA/RNA Shield (Zymo Research) or obtained from tissue scraped from settlement plugs that were snap-frozen in liquid nitrogen (Fig 1A). RNA and DNA extractions were performed with the Quick DNA/RNA Miniprep Plus Kit (Zymo Research Catalog #7003) according to the manufacturer's instructions (see protocol in data repository; (88)). We sequenced RNA using TagSeq, which is a 3' short transcript method that is a cost-effective alternative to RNAseq and allows for accurate estimates of transcript abundance (50). Library preparation was adapted for sequencing on one lane of Illumina NovaSeq 6000 SR100 with standard coverage of 3-5 million 100 bp single end reads (University of Texas Austin, Genomic Sequencing and Analysis Facility). Sequence reads were trimmed and filtered for quality control and aligned and mapped to the *M. capitata* reference assembly (93) to generate a gene count matrix (SI Appendix, Supplementary Methods). Gene expression across developmental time points was first visualized using a principal component analysis (PCA) and tested using a permutational analysis of variance (PERMANOVA) in the *vegan* package (94). Gene expression was then analyzed using a weighted gene co-expression network analysis (WGCNA) in the *WGCNA* package (52) and assigned to modules by expression pattern. Functional enrichment of genes in each module was conducted by analyzing the list of genes associated with each ontogenetic pattern using gene ontology (GO) enrichment analysis in GOSeq (95) and published functional annotation accompanying the reference genome (93). Significantly enriched GO terms

were filtered to select terms of interest related to carbohydrate metabolism, lipid metabolism, and communication and transport (SI Appendix, Supplementary Methods).

E. Metabolomics

Samples for metabolomic analysis were snap-frozen in liquid nitrogen and stored at -80°C (Fig 1A). Metabolites were extracted from the coral host fraction according to (51) and identified and quantified at the Rutgers Cancer Institute of New Jersey Metabolomics facility using hydrophilic interaction liquid chromatography separation and liquid chromatography-mass spectrometry (LC-MS) quantification (SI Appendix, Supplementary Methods). Ion counts for identified metabolites were center normalized to the respective sample median and $\log_{10}$ transformed. We examined metabolomic profiles across development using supervised partial least squares discriminant analysis (PLS-DA) in the *mixOmics* package (96). To detect metabolites that correlated with developmental time points, we conducted a weighted correlation network analysis (WCNA) in the *WGCNA* package (52) Metabolites were then analyzed for enrichment of compound class and KEGG pathways using the list of metabolites associated with each ontogenetic pattern in MetaboAnalyst v5.0 web interface (97).

F. ITS2 amplicon sequencing

ITS2 amplicon sequencing was conducted to identify Symbiodiniaceae communities from extracted DNA across time points (Fig 1A). A two-step PCR protocol was used to prepare PCR products for sequencing according to a modification of the Illumina 16S Metagenomic Sequencing Library Preparation protocol (see protocol in data repository; (88)) to amplify the ITS2 region of Symbiodiniaceae nuclear ribosomal DNA using published primers (98). Samples were sequenced on an Illumina MiSeq platform (Illumina, San Diego, CA) using 2x300 bp paired-end sequencing at the RI-INBRE Molecular Informatics Core (Kingston, RI). Sequences were quality controlled and subsampled to even sequencing depth and analyzed locally to identify Symbiodiniaceae Defining Intragenomic Variants (DIVs) that determine ITS2 type profiles using the SymPortal workflow (35). Relative abundance was calculated and visualized for DIVs at >1% relative abundance. Alpha diversity of DIVs was calculated using Shannon and Inverse Simpson indices and analyzed using one-way ANOVA with time point as the main effect. Shifts in Symbiodiniaceae communities (Bray-Curtis dissimilarity) were visualized across ontogeny using a non-metric multidimensional scaling analysis (NMDS) in the *phyloseq* package (99).

G. 16S rRNA amplicon sequencing

To identify microbial communities, we conducted 16S rRNA amplicon sequencing across development (Fig 1A). Extracted DNA was prepared using a two-step PCR protocol using published primers for the 16S rRNA V4 variable region (100). Samples were then sequenced on an Illumina MiSeq (Illumina, San Diego, CA) for 2x300 bp paired-end sequencing at the RI-INBRE Molecular Informatics Core. We conducted data analysis using the *mothur* analytical pipeline (v1.46.1) (101) including filtering, alignment to the Silva database (release 138.1; (102)), removal of chimeras, and subsampling (900 sequences) to quantify operational taxonomic units (OTU). Due to low bacterial sequences, 13 out of 39 samples were removed after subsampling. The removed samples included egg (1 hpf), embryo (5 hpf), and half of the samples at 38 and 65 hpf stages, indicating low bacterial sequences generated from the earliest life stages in the time series, which corresponded to samples with low DNA concentration during extraction. Shifts in bacterial communities (Bray-Curtis dissimilarity) across ontogeny were visualized using a non-metric multidimensional scaling analysis (NMDS) in the *phyloseq* package (99). Taxa abundance was calculated as percent relative abundance and filtered to those present at >0.5% for visualization at the genus level. Alpha diversity was calculated using Shannon and Inverse Simpson indices. Changes in alpha diversity across development were analyzed using a one-way ANOVA with time point as the main effect.

Acknowledgments

We are grateful for the logistical support provided by the Coral Resilience Lab and the Hawai□i Institute of Marine Biology. We acknowledge Margaret Schedl for RNA extraction, Craig Nelson and Shayle Matsuda for discussions on 16S bacterial analyses, David Beck for assistance with integrative analysis and computing, Eric Chiles and Xiaoyang Su for metabolomics discussions, and the Putnam (University of Rhode Island) and Roberts Labs (University of Washington) for feedback on earlier versions of this manuscript. We acknowledge use of the computational resources of the URI Center for Computational Research for this work. As guests, we recognize and give thanks for the land and water resources of the ʼāina and the traditional owners of the land, kānaka ʼōiwi, both past and present, as well as future generations, on which this experimental work was conducted in the Kāne□ohe Ahupuaʻa and the islands of Hawaiʻi.

Funding

This research was supported by the National Science Foundation Ocean Sciences Postdoctoral Fellowship to ASH (award no. 2205966), US-Israeli Binational Science Foundation to HMP and TM (award no. BSF 2016-321), National Science Foundation Rules of Life-Epigenetics (award no. EF-1921465) and a gift of the Washington Research Foundation to the University of Washington eScience Institute.

Data Availability

Data and scripts are available on GitHub at https://github.com/AHuffmyer/EarlyLifeHistory_Energetics/releases/tag/v1.0.0 and Open Science Framework (OSF) (88). Raw sequence files (TagSeq, ITS2, and 16S) are stored at the NCBI Sequence Read Archive under project PRJNA900235. Raw and processed metabolomic data are archived at OSF (88).

Author Contributions

Author contributions: A.S.H. and H.M.P. designed research; A.S.H. performed research and sample collection; A.S.H., K.H.W., D.M.B., and E.S. collected and analyzed data; A.S.H. wrote the manuscript and K.H.W, D.M.B., E.S., T.M., and H.M.P. revised the manuscript. All authors approved the final submission.

References

1. L. Muscatine, J. W. Porter, Reef Corals: Mutualistic Symbioses Adapted to Nutrient-Poor Environments. *Bioscience* **27**, 454–460 (1977).
2. T. C. LaJeunesse, *et al.*, Systematic revision of Symbiodiniaceae highlights the antiquity and diversity of coral endosymbionts. *Curr. Biol.* **28**, 2570–2580 (2018).
3. L. Muscatine, L. R. Mccloskey, R. E. Marian, Estimating the daily contribution of carbon from zooxanthellae to coral animal respiration. *Limnol. Oceanogr.* **26**, 601–611 (1981).
4. P. G. Falkowski, Z. Dubinsky, L. Muscatine, J. W. Porter, Light and the bioenergetics of a symbiotic coral. *Bioscience* **34**, 705–709 (2006).
5. P. G. Falkowski, Z. Dubinsky, L. Muscatine, L. McCloskey, Population control in symbiotic corals - Ammonium ions and organic materials maintain the density of zooxanthellae. *Bioscience* **43**, 606–611 (1993).
6. S. Roberty, E. Béraud, R. Grover, C. Ferrier-Pagès, Coral Productivity Is Co-Limited by Bicarbonate and Ammonium Availability. *Microorganisms* **8** (2020).
7. D. G. Bourne, K. M. Morrow, N. S. Webster, Insights into the Coral Microbiome: Underpinning the Health and Resilience of Reef Ecosystems. *Annu. Rev. Microbiol.* **70**, 317–340 (2016).
8. S. R. Connolly, D. R. Bellwood, T. P. Hughes, Indo-pacific biodiversity of coral reefs:

Deviations from a mid-domain model. *Ecology* **84**, 2178–2190 (2003).
9. A. J. Woodhead, C. C. Hicks, A. V. Norström, G. J. Williams, N. A. J. Graham, Coral reef ecosystem services in the Anthropocene. *Funct. Ecol.* (2019) https:/doi.org/10.1111/1365-2435.13331.
10. V. M. Weis, Cellular mechanisms of Cnidarian bleaching: stress causes the collapse of symbiosis. *J. Exp. Biol.* **211**, 3059–3066 (2008).
11. S. Sully, D. E. Burkepile, M. K. Donovan, G. Hodgson, R. van Woesik, A global analysis of coral bleaching over the past two decades. *Nat. Commun.* **10**, 1264 (2019).
12. T. D. Eddy, *et al.*, Global decline in capacity of coral reefs to provide ecosystem services. *One Earth* **4**, 1278–1285 (2021).
13. R. Ritson-Williams, *et al.*, New perspectives on ecological mechanisms affecting coral recruitment on reefs. *Smithson. Contrib. Mar. Sci.* **38**, 437–457 (2009).
14. J. Pineda, Linking larval settlement to larval transport: assumptions, potentials, and pitfalls. *Oceanography of the eastern Pacific* **1**, 84–105 (2000).
15. D. J. Marshall, A. K. Pettersen, M. Bode, C. R. White, Developmental cost theory predicts thermal environment and vulnerability to global warming. *Nature Ecology and Evolution* **4**, 406–411 (2020).
16. A. H. Baird, J. R. Guest, B. L. Willis, Systematic and Biogeographical Patterns in the Reproductive Biology of Scleractinian Corals. *Annu. Rev. Ecol. Evol. Syst.* **40**, 551–571 (2009).
17. S. L. Rosset, *et al.*, The Molecular Language of the Cnidarian–Dinoflagellate Symbiosis. *Trends Microbiol.* **29**, 320-333 (2021).
18. S. Harii, K. Nadaoka, M. Yamamoto, K. Iwao, Temporal changes in settlement, lipid content and lipid composition of larvae of the spawning hermatypic coral Acropora tenuis. *Mar. Ecol. Prog. Ser.* **346**, 89–96 (2007).
19. J. Figueiredo, *et al.*, Ontogenetic change in the lipid and fatty acid composition of scleractinian coral larvae. *Coral Reefs* **31**, 613–619 (2012).
20. M. R. Gaither, R. Rowan, Zooxanthellar symbiosis in planula larvae of the coral *Pocillopora damicornis*. *J. Exp. Mar. Bio. Ecol.* **386**, 45–53 (2010).
21. S. Harii, M. Yamamoto, O. Hoegh-Guldberg, The relative contribution of dinoflagellate photosynthesis and stored lipids to the survivorship of symbiotic larvae of the reef-building corals. *Mar. Biol.* **157**, 1215–1224 (2010).
22. C. Kopp, I. Domart-Coulon, D. Barthelemy, A. Meibom, Nutritional input from dinoflagellate symbionts in reef-building corals is minimal during planula larval life stage. *Sci Adv* **2**, e1500681 (2016).
23. B. Nesa, A. H. Baird, S. Harii, I. Yakovleva, M. Hidaka, Algal symbionts increase DNA damage in coral planulae exposed to sunlight. *Zool. Stud.* **51**, 6 (2012).
24. M. Mies, P. Y. G. Sumida, N. Rädecker, C. R. Voolstra, Marine Invertebrate Larvae Associated with *Symbiodinium*: A Mutualism from the Start? *Frontiers in Ecology and Evolution* **5**, 56 (2017).
25. B. Mos, S. A. Dworjanyn, Early metamorphosis is costly and avoided by young, but physiologically competent, marine larvae. *Mar. Ecol. Prog. Ser.* **559**, 117–129 (2016).
26. J. A. Pechenik, Larval experience and latent effects--metamorphosis is not a new beginning. *Integr. Comp. Biol.* **46**, 323–333 (2006).
27. P. J. Edmunds, V. R. Cumbo, T.-Y. Fan, Metabolic costs of larval settlement and metamorphosis in the coral *Seriatopora caliendrum* under ambient and elevated pCO2. *J. Exp. Mar. Bio. Ecol.* **443**, 33–38 (2013).
28. N. Radecker, C. Pogoreutz, C. R. Voolstra, J. Wiedenmann, C. Wild, Nitrogen cycling in corals: The key to understanding holobiont functioning? *Trends Microbiol.* **23**, 490–497 (2015).
29. L. Allen-Waller, K. L. Barott, Symbiotic dinoflagellates divert energy away from mutualism during coral bleaching recovery. *Symbiosis* (2023) https:/doi.org/10.1007/s13199-023-00901-3.
30. C. B. Wall, M. Kaluhiokalani, B. N. Popp, M. J. Donahue, R. D. Gates, Divergent symbiont communities determine the physiology and nutrition of a reef coral across a light-availability

gradient. *ISME J.* **14**, 945–958 (2020).
31. M. Helmkampf, M. R. Bellinger, M. Frazier, M. Takabayashi, Symbiont type and environmental factors affect transcriptome-wide gene expression in the coral *Montipora capitata*. *Ecol. Evol.* **9**, 378–392 (2019).
32. R. Cunning, R. Ritson-Williams, R. D. Gates, Patterns of bleaching and recovery of *Montipora capitata* in Kane'ohe Bay, Hawai'i, USA. *Mar. Ecol. Prog. Ser.* **551**, 131–139 (2016).
33. T. C. LaJeunesse, D. J. Thornhill, Improved resolution of reef-coral endosymbiont (*Symbiodinium*) species diversity, ecology, and evolution through psbA non-coding region genotyping. *PLoS One* **6**, e29013 (2011).
34. D. C. Wham, G. Ning, T. C. LaJeunesse, *Symbiodinium glynnii* sp. nov., a species of stress-tolerant symbiotic dinoflagellates from pocilloporid and montiporid corals in the Pacific Ocean. *Phycologia* **56**, 396–409 (2017).
35. B. C. C. Hume, *et al.*, SymPortal: A novel analytical framework and platform for coral algal symbiont next-generation sequencing ITS2 profiling. *Mol. Ecol. Resour.* **19**, 1063–1080 (2019).
36. T. N. F. Roach, J. H. Dilworth, C. Martin H., A. Daniel Jones, R. A. Quinn, C. Drury, Metabolomic signatures of coral bleaching history. *Nat. Ecol. Evol.* **5**, 495-503 (2021).
37. J. Dilworth, C. Caruso, V. A. Kahkejian, A. C. Baker, C. Drury, Host genotype and stable differences in algal symbiont communities explain patterns of thermal stress response of Montipora capitata following thermal pre-exposure and across multiple bleaching events. *Coral Reefs* **40**, 151–163 (2021).
38. J. L. Padilla-Gamiño, X. Pochon, C. Bird, G. T. Concepcion, R. D. Gates, From parent to gamete: vertical transmission of *Symbiodinium* (Dinophyceae) ITS2 sequence assemblages in the reef building coral *Montipora capitata*. *PLoS One* **7**, e38440 (2012).
39. K. H. Sharp, K. B. Ritchie, Multi-partner interactions in corals in the face of climate change. *Biol. Bull.* **223**, 66–77 (2012).
40. J. L. Matthews, *et al.*, Symbiodiniaceae-bacteria interactions: rethinking metabolite exchange in reef-building corals as multi-partner metabolic networks. *Environ. Microbiol.* **22**, 1675–1687 (2020).
41. J. Ceh, *et al.*, Nutrient cycling in early coral life stages: *Pocillopora damicornis* larvae provide their algal symbiont (*Symbiodinium*) with nitrogen acquired from bacterial associates. *Ecol. Evol.* **3**, 2393–2400 (2013).
42. A. D. Williams, B. E. Brown, L. Putchim, M. J. Sweet, Age-Related Shifts in Bacterial Diversity in a Reef Coral. *PLoS One* **10**, e0144902 (2015).
43. N. E. Kimes, J. D. Van Nostrand, E. Weil, J. Zhou, P. J. Morris, Microbial functional structure of *Montastraea faveolata*, an important Caribbean reef-building coral, differs between healthy and yellow-band diseased colonies. *Environ. Microbiol.* **12**, 541–556 (2010).
44. J.-B. Raina, E. A. Dinsdale, B. L. Willis, D. G. Bourne, Do the organic sulfur compounds DMSP and DMS drive coral microbial associations? *Trends Microbiol.* **18**, 101–108 (2010).
45. H. G. Reich, E. F. Camp, L. M. Roger, H. M. Putnam, The trace metal economy of the coral holobiont: supplies, demands and exchanges. *Biol. Rev.* **98**, 623-642 (2022).
46. J.-B. Raina, *et al.*, Isolation of an antimicrobial compound produced by bacteria associated with reef-building corals. *PeerJ* **4**, e2275 (2016).
47. A. Cárdenas, *et al.*, Greater functional diversity and redundancy of coral endolithic microbiomes align with lower coral bleaching susceptibility. *ISME J.* **16**, 2406–2420 (2022).
48. E. M. Sogin, H. M. Putnam, C. E. Nelson, P. Anderson, R. D. Gates, Correspondence of coral holobiont metabolome with symbiotic bacteria, archaea and *Symbiodinium* communities. *Environ. Microbiol. Rep.* **9**, 310–315 (2017).
49. J. P. Engelberts, S. J. Robbins, K. Damjanovic, N. S. Webster, Integrating novel tools to elucidate the metabolic basis of microbial symbiosis in reef holobionts. *Mar. Biol.* **168**, 175 (2021).
50. B. K. Lohman, J. N. Weber, D. I. Bolnick, Evaluation of TagSeq, a reliable low-cost alternative for RNAseq. *Mol. Ecol. Resour.* **16**, 1315–1321 (2016).
51. A. Williams, *et al.*, Metabolomic shifts associated with heat stress in coral holobionts. *Sci*

Adv **7**, eabd4210 (2021).
52. P. Langfelder, S. Horvath, WGCNA: an R package for weighted correlation network analysis. *BMC Bioinformatics* **9**, 559 (2008).
53. E. Chille, *et al.*, Developmental series of gene expression clarifies maternal mRNA provisioning and maternal-to-zygotic transition in a reef-building coral. *BMC Genomics* **22**, 815 (2021).
54. Y. H. Fadlallah, Coral Reefs Sexual Reproduction, Development and Larval Biology in Scleractinian Corals: A Review. *Coral Reefs* **2**, 129–150 (1983).
55. S. Ghosh, A. Körte, G. Serafini, V. Yadav, J. Rodenfels, Developmental energetics: Energy expenditure, budgets and metabolism during animal embryogenesis. *Semin. Cell Dev. Biol.* **138**, 83-93 (2022).
56. M. E. Strader, G. V. Aglyamova, M. V. Matz, Molecular characterization of larval development from fertilization to metamorphosis in a reef-building coral. *BMC Genomics* **19**, 17 (2018).
57. L. J. Rodrigues, J. L. Padilla-Gamiño, Trophic provisioning and parental trade-offs lead to successful reproductive performance in corals after a bleaching event. *Sci. Rep.* **12**, 18702 (2022).
58. S. E. Leinbach, K. E. Speare, A. M. Rossin, D. M. Holstein, M. E. Strader, Energetic and reproductive costs of coral recovery in divergent bleaching responses. *Sci. Rep.* **11**, 23546 (2021).
59. S. K. Davy, D. Allemand, V. M. Weis, Cell biology of cnidarian-dinoflagellate symbiosis. *Microbiol. Mol. Biol. Rev.* **76**, 229–261 (2012).
60. J. L. Matthews, *et al.*, Partner switching and metabolic flux in a model cnidarian-dinoflagellate symbiosis. *Proc. Biol. Sci.* **285**, 20182336 (2018).
61. D. Yellowlees, T. A. V. Rees, W. Leggat, Metabolic interactions between algal symbionts and invertebrate hosts. *Plant Cell Environ.* **31**, 679–694 (2008).
62. A. A. Venn, J. E. Loram, A. E. Douglas, Photosynthetic symbioses in animals. *J. Exp. Bot.* **59**, 1069–1080 (2008).
63. M. S. Burriesci, T. K. Raab, J. R. Pringle, Evidence that glucose is the major transferred metabolite in dinoflagellate-cnidarian symbiosis. *J. Exp. Biol.* **215**, 3467–3477 (2012).
64. M. A. Teece, B. Estes, E. Gelsleichter, D. Lirman, Heterotrophic and autotrophic assimilation of fatty acids by two scleractinian corals, *Montastraea faveolate* and *Porites astreoides*. *Limnol. Oceanogr.* **56**, 1285–1296 (2011).
65. C. Treignier, I. Tolosa, R. Grover, S. Reynaud, C. Ferrier-Pagés, Carbon isotope composition of fatty acids and sterols in the scleractinian coral *Turbinaria reniformis*: Effect of light and feeding. *Limnol. Oceanogr.* **54**, 1933–1940 (2009).
66. E. M. Lehnert, *et al.*, Extensive differences in gene expression between symbiotic and aposymbiotic cnidarians. *G3* **4**, 277–295 (2014).
67. V. Z. Radice, *et al.*, Evaluating coral trophic strategies using fatty acid composition and indices. *PLoS One* **14**, e0222327 (2019).
68. L. A. Morris, C. R. Voolstra, K. M. Quigley, D. G. Bourne, L. K. Bay, Nutrient Availability and Metabolism Affect the Stability of Coral–Symbiodiniaceae Symbioses. *Trends Microbiol.* **27**, 678–689 (2019).
69. O. Rahav, Z. Dubinsky, Y. Achituv, P. G. Falkowski, D. C. Smith, Ammonium metabolism in the zooxanthellate coral, *Stylophora pistillata*. *Proc. Royal Soc. B.* **236**, 325–337 (1989).
70. J. L. Matthews, *et al.*, Optimal nutrient exchange and immune responses operate in partner specificity in the cnidarian-dinoflagellate symbiosis. *Proc. Natl. Acad. Sci. U.S.A.* **114**, 13194–13199 (2017).
71. S. Levy, *et al.*, A stony coral cell atlas illuminates the molecular and cellular basis of coral symbiosis, calcification, and immunity. *Cell* **184**, 2973–2987.e18 (2021).
72. S. A. Kitchen, V. M. Weis, The sphingosine rheostat is involved in the cnidarian heat stress response but not necessarily in bleaching. *J. Exp. Biol.* **220**, 1709–1720 (2017).
73. A. Bertucci, S. Forêt, E. E. Ball, D. J. Miller, Transcriptomic differences between day and night in *Acropora millepora* provide new insights into metabolite exchange and light-enhanced calcification in corals. *Mol. Ecol.* **24**, 4489–4504 (2015).

74. E. M. Hemond, S. V. Vollmer, Diurnal and nocturnal transcriptomic variation in the Caribbean staghorn coral, *Acropora cervicornis*. *Mol. Ecol.* **24**, 4460–4473 (2015).
75. M. Neder, R. Saar, A. Malik, G. Antler, T. Mass, New Insights on the Diurnal Mechanism of Calcification in the Stony Coral, *Stylophora pistillata*. *Frontiers in Marine Science* **8** (2022).
76. M. E. Strader, J. M. Wong, G. E. Hofmann, Ocean acidification promotes broad transcriptomic responses in marine metazoans: a literature survey. *Front. Zool.* **17**, 7 (2020).
77. K. E. Hillyer, S. Tumanov, S. Villas-Bôas, S. K. Davy, Metabolite profiling of symbiont and host during thermal stress and bleaching in a model cnidarian-dinoflagellate symbiosis. *J. Exp. Biol.* **219**, 516–527 (2016).
78. C. Kopp, *et al.*, Subcellular investigation of photosynthesis-driven carbon assimilation in the symbiotic reef coral *Pocillopora damicornis*. *MBio* **6** (2015).
79. N.-R. Kochman, R. Grover, C. Rottier, C. Ferrier-Pages, M. Fine, The reef building coral *Stylophora pistillata* uses stored carbohydrates to maintain ATP levels under thermal stress. *Coral Reefs* **40**, 1473-1485 (2021).
80. D. Zoccola, *et al.*, Bicarbonate transporters in corals point towards a key step in the evolution of cnidarian calcification. *Sci. Rep.* **5**, 9983 (2015).
81. J. T. Wang, A. E. Douglas, Essential amino acid synthesis and nitrogen recycling in an alga-invertebrate symbiosis. *Mar. Biol.* **135**, 219–222 (1999).
82. A. H. Baird, I. M. Yakovleva, S. Harii, F. Sinniger, M. Hidaka, Environmental constraints on the mode of symbiont transmission in corals. *J. Exp. Mar. Bio. Ecol.* **538**, 151499 (2021).
83. I. M. Yakovleva, *et al.*, Algal symbionts increase oxidative damage and death in coral larvae at high temperatures. *Mar. Ecol. Prog. Ser.* **378**, 105–112 (2009).
84. J. M. McDevitt-Irwin, J. K. Baum, M. Garren, R. L. Vega Thurber, Responses of Coral-Associated Bacterial Communities to Local and Global Stressors. *Front. Mar. Sci.* **4** (2017).
85. S. A. Gignoux-Wolfsohn, S. V. Vollmer, Identification of Candidate Coral Pathogens on White Band Disease-Infected Staghorn Coral. *PLoS One* **10**, e0134416 (2015).
86. D. Meron, *et al.*, Changes in coral microbial communities in response to a natural pH gradient. *ISME J.* **6**, 1775–1785 (2012).
87. H. Jorissen, *et al.*, Coral larval settlement preferences linked to crustose coralline algae with distinct chemical and microbial signatures. *Scientific Reports* **11**, 14610 (2021).
88. A. S. Huffmyer, Cross-scale and multi-omic integration reveals transitions to symbiotic nutritional integration across coral ontogeny. Available at https:/doi.org/10.17605/OSF.IO/KMU7H (2023)
89. E. M. Gibbin, H. M. Putnam, R. D. Gates, M. R. Nitschke, S. K. Davy, Species-specific differences in thermal tolerance may define susceptibility to intracellular acidosis in reef corals. *Mar. Biol.* **162**, 717–723 (2015).
90. J. Fox, S. Weisberg, *An R Companion to Applied Regression*, Second (SAGE Publications, 2018).
91. R Core Team, *R: A language and environment for statistical computing* (R Foundation for Statistical Computing, 2022).
92. C. T. Rueden, *et al.*, ImageJ2: ImageJ for the next generation of scientific image data. *BMC Bioinformatics* **18**, 529 (2017).
93. T. G. Stephens, *et al.*, High-quality genome assembles from key Hawaiian coral species. *Gigascience* **11** (2022).
94. J. Okansen, et al., *vegan: Community Ecology Package* (2017).
95. M. D. Young, M. J. Wakefield, G. K. Smyth, A. Oshlack, Gene ontology analysis for RNA-seq: accounting for selection bias. *Genome Biol.* **11**, R14 (2010).
96. F. Rohart, B. Gautier, A. Singh, K.-A. Lê Cao, mixOmics: An R package for ’omics feature selection and multiple data integration. *PLoS Comput. Biol.* **13**, e1005752 (2017).
97. Z. Pang, *et al.*, MetaboAnalyst 5.0: narrowing the gap between raw spectra and functional insights. *Nucleic Acids Res.* **49**, W388–W396 (2021).
98. T. C. Lajeunesse, R. K. Trench, Biogeography of two species of *Symbiodinium* (Freudenthal) inhabiting the intertidal sea anemone *Anthopleura elegantissima* (Brandt). *Biol. Bull.* **199**, 126–134 (2000).
99. P. J. McMurdie, S. Holmes, phyloseq: an R package for reproducible interactive analysis

and graphics of microbiome census data. *PLoS One* **8**, e61217 (2013).
100. A. Apprill, S. McNally, R. Parsons, L. Weber, Minor revision to V4 region SSU rRNA 806R gene primer greatly increases detection of SAR11 bacterioplankton. *Aquat. Microb. Ecol.* **75**, 129–137 (2015).
101. P. D. Schloss, *et al.*, Introducing *mothur*: open-source, platform-independent, community-supported software for describing and comparing microbial communities. *Appl. Environ. Microbiol.* **75**, 7537–7541 (2009).
102. C. Quast, *et al.*, The SILVA ribosomal RNA gene database project: improved data processing and web-based tools. *Nucleic Acids Res.* **41**, D590–6 (2013).

Figures and Tables

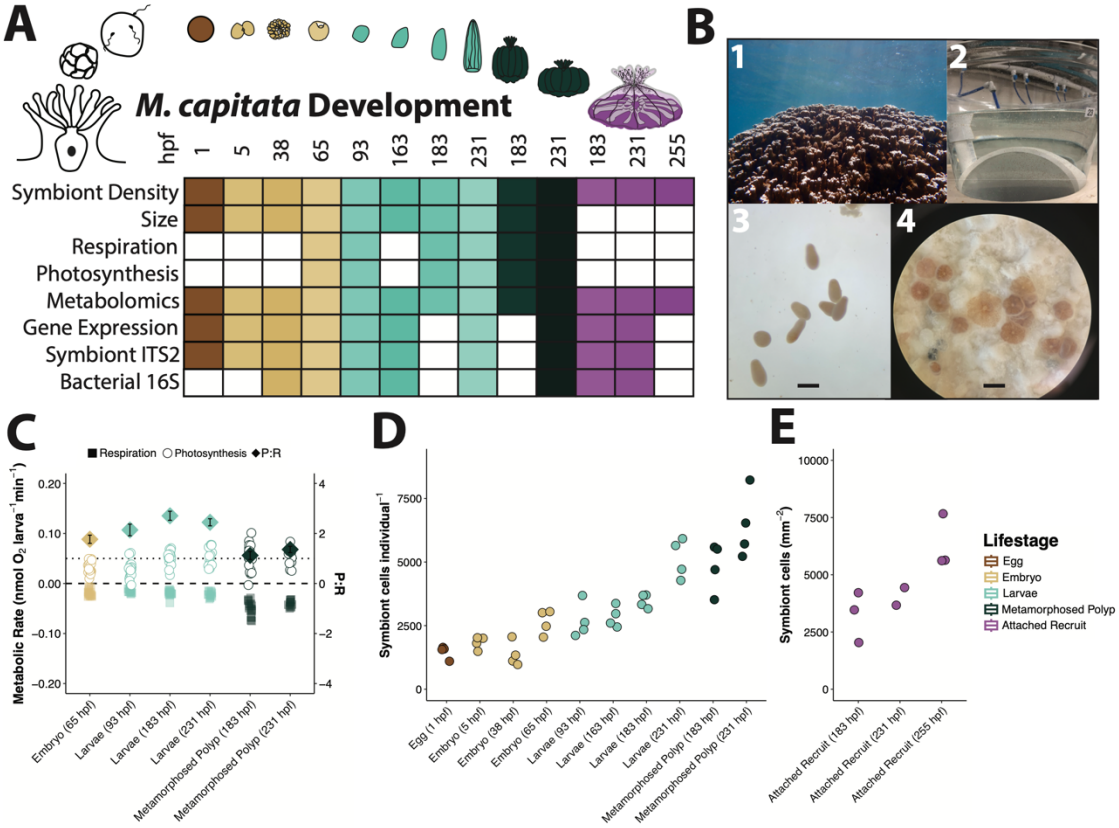

Figure 1. Study overview and physiological responses across ontogeny. (A) Variables measured across *Montipora capitata* development. Filled squares indicate response variable was sampled at the respective time point; white squares indicate the response was not measured or data is not available. Color corresponds to major life history grouping (eggs=brown, embryos=yellow, larvae=cyan, metamorphosed polyps=green, attached recruits=pink). hpf indicates hours-post-fertilization. (B) Photographs of 1 – *M. capitata* colony; 2 - Conical larval rearing chambers, photo credit: Josh Hancock; 3 - Planula larvae, note pigmentation due to presence of symbiont cells, scale bar indicates 1 mm; 4 - Close up image of attached recruits on settlement plug, scale bar indicates 1 mm. (C) Respiration (filled squares; oxygen consumed (note that lower values indicate higher oxygen consumption); µmol O_2 larva^{-1} min^{-1}), gross photosynthesis (open circles; oxygen produced; µmol O_2 larva^{-1} min^{-1}), and photosynthesis:respiration ratio (closed diamonds; oxygen produced:oxygen consumed; P:R on the secondary y-axis) during development in *M. capitata*. P:R displayed as mean ± standard error of mean. Dashed line is plotted at zero on the y axis; dotted line indicates P:R ratio of 1:1. Developmental time point indicated on the x axis with colors indicating life stage. (D) Symbiont cells per individual across development in eggs through metamorphosed polyps. (E) Symbiont cells per mm^2 surface area in attached recruits.

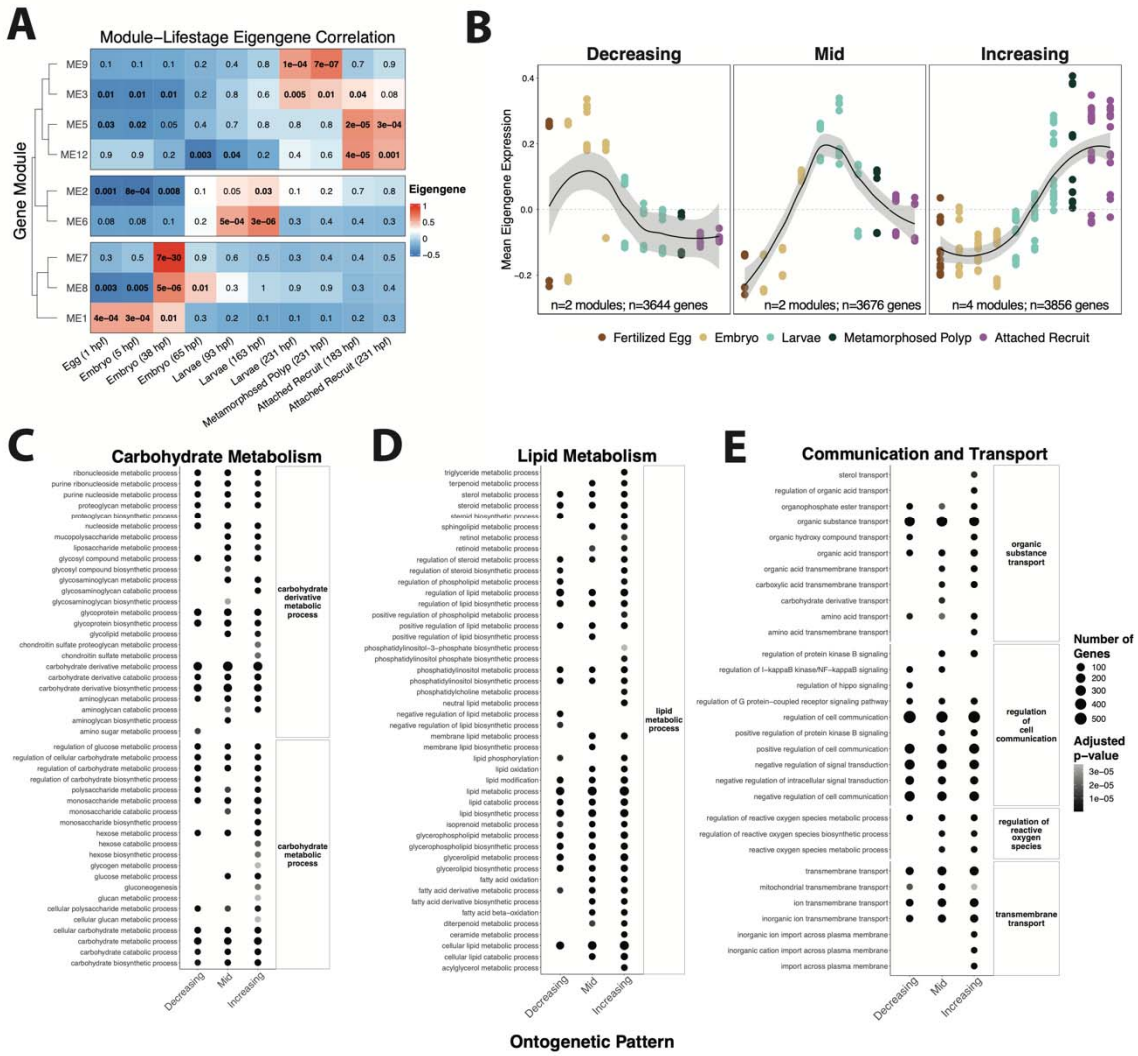

Figure 2. Gene expression across *Montipora capitata* ontogeny. (A) WGCNA analysis with modules of genes (y axis) with positive eigengene expression (red) and negative expression (blue) correlated with life stage (x axis). Bold values indicate a module is significantly related to the respective life stage ($P<0.05$). (B) Modules were characterized by the ontogenetic pattern of eigengene expression (y axis) - decreasing across development, peaking in mid-development, or increasing across development. Life stage groupings indicated by colors (eggs=brown, embryos=yellow, larvae=cyan, metamorphosed polyps=green, attached recruits=pink). Trends lines were plotted using the loess method. Genes in modules of each ontogenetic pattern were functionally annotated using GOSeq at Biological Process ontology. Significantly enriched GO terms ($P<0.001$) displayed for terms related to (C) carbohydrate metabolism, (D) lipid metabolism, and (E) communication and transport. Point size indicates number of genes included in category; color indicates adjusted p-value.

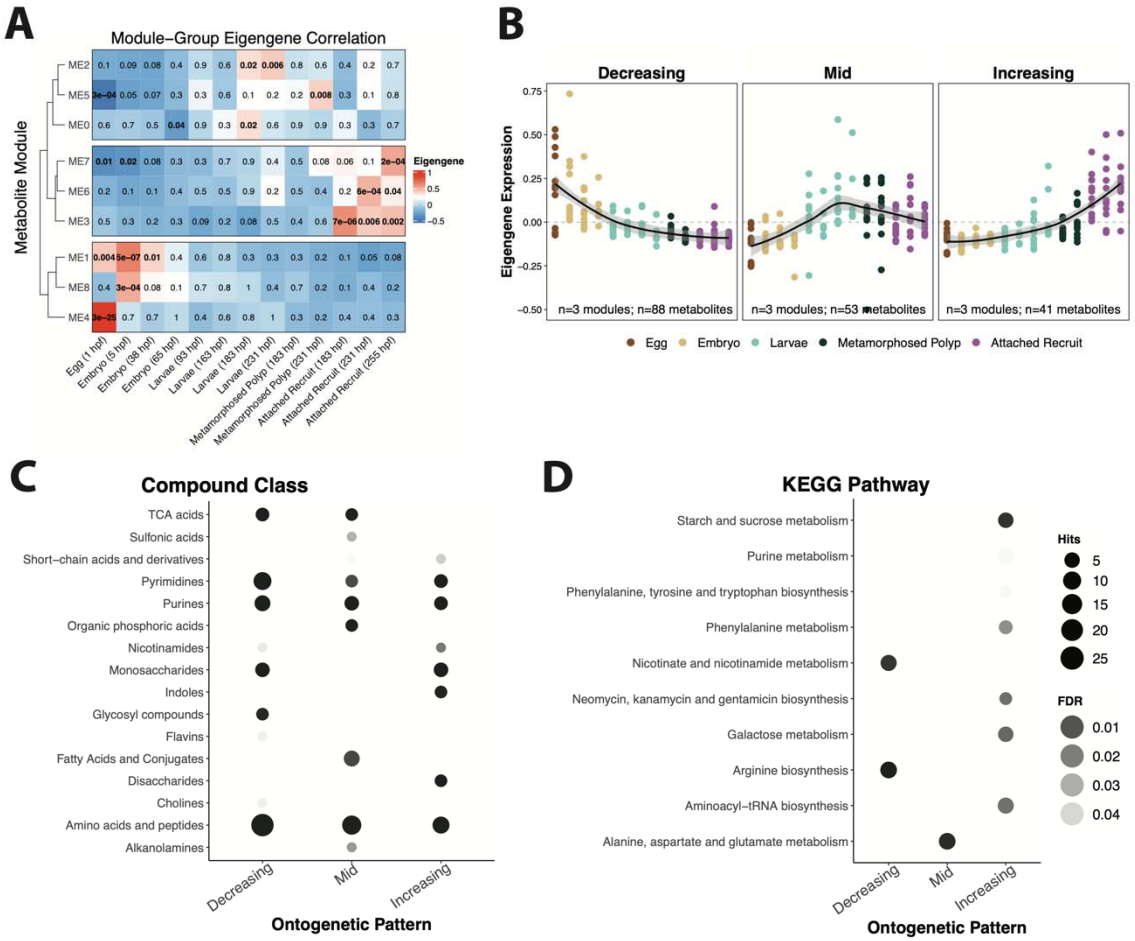

Figure 3. Metabolomics across *Montipora capitata* ontogeny. (A) WCNA analysis with modules of metabolites (y axis) with positive eigengene expression (red) and negative expression (blue) correlated with life stage (x axis). Bold values indicate a module is significantly related to the respective life stage (*P*<0.05). (B) Modules were characterized by ontogenetic pattern of eigengene expression (y axis) - decreasing across development, peaking in mid-development, or increasing across development. Life stage groupings indicated by colors (eggs=brown, embryos=yellow, larvae=cyan, metamorphosed polyps=green, attached recruits=pink). Trends were plotted using the loess method. Metabolites in modules of each ontogenetic pattern were functionally annotated to (C) compound classes and (D) KEGG pathway levels. Point size indicates number of metabolites ("Hits") included in category; color indicates adjusted p-value.

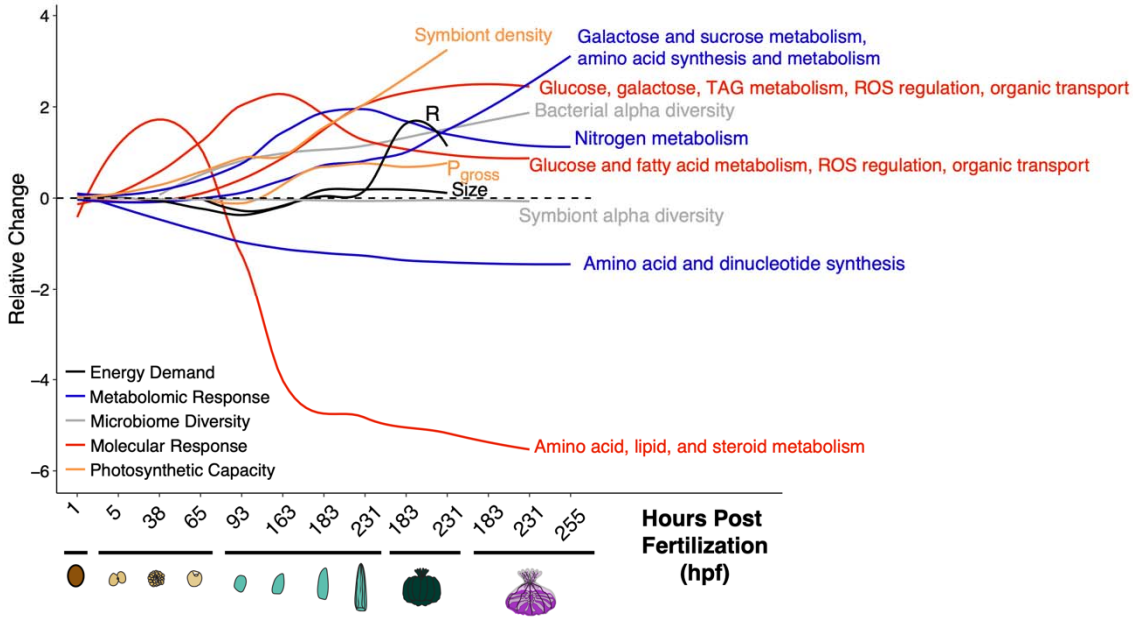

Figure 4. Relative change in response variables across a *Montipora capitata* developmental time series. Responses are characterized as energy demand (black; size and respiration), metabolomic responses (blue; metabolomic ontogenetic patterns with key functional enrichment terms), molecular responses (red; gene expression ontogenetic patterns with key functional enrichment terms), microbiome diversity (gray; Symbiodiniaceae ITS2 alpha diversity and bacterial 16S alpha diversity), and photosynthetic capacity (orange; gross photosynthesis [P gross] and symbiont density). Loess lines were plotted to indicate trends across life stages. Dashed line indicates no relative change. Relative change calculated from the earliest available life stage in each data set. TAG = triacylglycerides.